科学出版社 出版
中国地理学会环境遥感分会
中国科学院遥感与数字地球研究所 主办

JOURNAL OF REMOTE SENSING
遥感学报

2013年 Vol.17 第17卷 No.4 第4期 ISSN 1007-4619 CN11-3841 / TP CODEN YXAUAB

2010年中国土地覆被遥感监测数据集（ChinaCover2010）

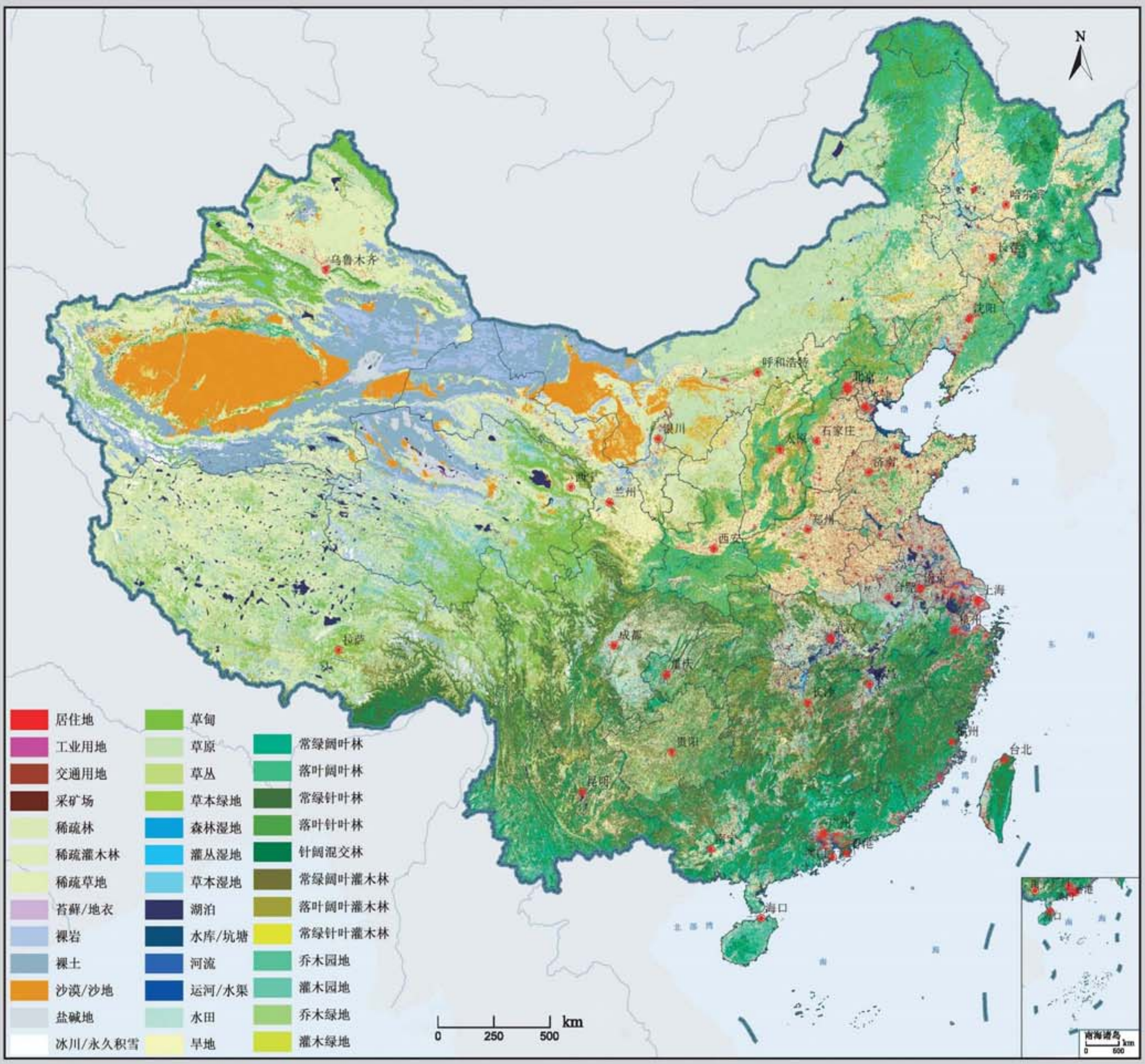

百种中国杰出学术期刊

遥感学报

Yaogan Xuebao

第 17 卷　第 4 期　2013 年 7 月

目　次

综述

基础理论

技术方法

遥感应用

“灰霾遥感”专栏

JOURNAL OF REMOTE SENSING

(**Vol. 17 No. 4 July, 2013**)

CONTENTS

(to be continued to Inside Back Cover)

(continued from Contents page)

Haze: Remote Sensing

Improved split window algorithm to retrieve LST from Terra/MODIS data

RI Changin[1,2], LIU Qinhuo[1], LI Hua[1], FANG Li[1], YU Yunyue[3], SUN Donglian[4]

1. *State Key Laboratory of Remote Sensing Science, Jointly Sponsored by the Institute of Remote Sensing and Digital Earth of Chinese Academy of Sciences and Beijing Normal University, Beijing* 100101, *China*;
2. *Laboratory of Digital Image Processing, Institute of Remote Sensing and Geo-informatics, State Academy of Sciences, Pyongyang, DPR Korea*;
3. *National Environmental Satellite, Data, and Information Service Center for Satellite Applications and Research, National Oceanic and Atmospheric Administration, Camp Springs, MD* 20746, *USA*;
4. *Department of Geography and Geoinformation Science, George Mason University, Fairfax, VA* 22030, *USA*

Abstract: This paper presents an algorithm for the retrieval of daytime land surface temperature (LST) from the Terra/MODIS data, which considers the atmospheric radiation effects due to the viewing zenith angle (VZA) variation. The MODTRAN4 model, 875 profiles of TIGR3 database and 106 surface emissivity spectra of the ASTER spectral library were used to obtain the Split-Window Algorithm (SWA) coefficients. The Root Mean Square Errors (RMSEs) of LST retrieval using the MODTRAN4 simulation are 0.34 K. Sensitivity analysis confirmed that the algorithm is not sensitive to total column water vapor content (TCWVC) for the moderately moist atmospheric conditions. In addition, LST retrieval error due to the VZA effect was reduced. Retrieved LSTs have compared with Mao, et al.'s LST and MOD11_L2 LST. Surface Radiation (SURFRAD) budget network measurements have been used for LST validation over six sites during the entire month of June 2009. The RMSE values of LST were 0.93 K, 1.49 K and 1.0 K for this new algorithm, Mao, et al.'s algorithm and MOD11_L2 LST, while the average biases were −0.66 K, 1.34 K and −0.38 K, respectively.

Key words: land surface temperature, split-window algorithm, MODIS, SURFRAD

CLC number: TP79 **Document code**: A

Citation format: **Ri C G, Liu Q H, Li H, Fang L, Yu Y Y and Sun D L. 2013. Improved split window algorithm to retrieve LST from Terra/MODIS data. Journal of Remote Sensing, 17(4): 830–840 [DOI: 10.11834/jrs.20132146]**

1 INTRODUCTION

LST is one of the most important parameters in surface-atmosphere interactions and energy flux between the surface and the atmosphere. In particular, it plays an important role in many applications such as agriculture, geosciences, climate science, and other environmental fields (Wan & Dozier, 1996). Thermal infrared (TIR) remote sensing is a unique way to obtain LST at regional or global land scales with different spatial resolutions and temporal scales.

Coll and Vicente (1997) developed a radiative transfer equation (RTE) for the LST retrieval by considering the Viewing Zenith Angle (VZA) effect and ground emissivity, but this model required a prior knowledge of TCWVC in addition to transmittance and surface emissivity. Another method of LST retrieval based on TCWVC estimate using the Split-Window Covariance Variance Ratio (SWCVR) has been introduced (Jedlovec, 1990; Sobrino, et al., 1996); however, it also requires a prior atmospheric transmittance. Li and Becker (1993) developed a method to estimate both land surface emissivity and LST using pairs of day/night co-registered AVHRR images, which also needs the atmosphere profile information. Wan & Dozier (1996) proposed a generalized SWA, which takes into account of the VZA effect and several intervals of LST and offers high accuracy of LST retrieval. But a prior knowledge of TCWVC is required for the coefficient estimate of the SWA. Wan and Li (1997) proposed a multi-band algorithm to retrieve land-surface emissivity and LST together from MODIS data, and the result is only influenced by

Received: 2012-04-28; **Accepted**: 2013-03-22; **Version of record first published**: 2013-03-29

Foundation: National Natural Science Foundation of China (No.40730525, 41101325, 41171282); National High Technology Research and Development Program of China (No.2012AA12A304); European Commission (Call FP7-ENV-2007-1, No. 212921) as part of the CEOP/AEGIS project.

First author biography: RI Changin (1972—), male, Ph.D. candidate. His research interests are land surface emissivity and temperature retrieval. E-mail: richangin@gmail.com

Corresponding author biography: LIU Qinhuo (1968—), male, Ph.D., professor. His research interests are radiation transfer model of land surface, quantitative remote sensing inversion, assimilation and applications. E-mail: qhliu@irsa.ac.cn

the surface optical properties and the ranges of atmospheric condition. Wan, et al. (2002, 2004) validated that the accuracy of these two algorithms is within 1 K. The accuracy of most algorithms is very high but they still need to make assumptions regarding prior knowledge of the atmosphere, especially water vapor content. Qin, et al. (2001) simplified the RTE to propose a SWA that needs only two parameters (emissivity and transmittance) and an accuracy under 2 K was observed. They developed a method to compute the transmittance from TCWVC, but it still requires a prior knowledge of TCWVC, which often is obtained from a meteorology station. Based on Qin, et al. (2001), Mao, et al. (2005) established a method to estimate the atmospheric transmittances using MODIS 31/32 and proposed a practical SWA for the LST retrieval. Moreover, for MODIS data, the linear simplification of Planck radiance in the whole range of BT regardless of atmospheric conditions was performed to avoid complicate calculation. The VZA effect related to a 55° scan angle of MODIS data affects the LST retrieval due to the change of atmospheric transmittance in MODIS 31/32, and thus, it is necessary to consider this effect in the RTE. In addition, the simulation between the atmospheric transmittance and TCWVC was carried out using the MODTRAN4 model only for the mid-latitude standard atmospheric conditions, which did not consider the global variability of the atmosphere. The assumption that atmospheric transmittance of upward radiance can be substituted for that of downward radiance causes some errors of LST retrieval due to the VZA effect. The linear simplification of the Planck's law in Mao, et al. (2005) can cause LST error due to the nonlinearity of the Planck function over the whole temperature range. Besides, the linear simplification in every separated temperature range can also introduce error because each range of temperature is generally different from the LST (T_s) and the average effective atmospheric temperature (T_a). Therefore, some efforts to eliminate these errors should be added in the SWA development. Meanwhile, some researchers have analyzed the effect of LST error for the VZA change to estimate numerical coefficients of SWA by considering its effect using the MODTRAN4 model from two thermal channels of different sensors (Yu, et al., 2009; Atitar & Sobrino, 2009; Jiang & Li, 2008; Tang, et al., 2008). Although the sensors used are different, these algorithms are similar in that they all consider the LST error due to a change in the VZA. In any case, the characteristics of the surface must be well known in advance (via the emissivity, or the land cover type and amount of vegetation cover) in order to obtain the LST, which is the main drawback of the SWA. For this reason, SWAs are typically working better for densely vegetated areas and water surfaces with known emissivities, but have known problems over semi-arid and arid regions where the emissivity is highly variable, both spatially and spectrally.

The objective of this paper is to propose an improved SWA which considers the atmospheric effect caused by the VZA change and performs the Planck's function simplification of the at-surface and effective atmospheric radiance in each sub-range of BT using the MODTRAN4 model with the Thermodynamic Initial Guess Retrieval (TIGR) database (Scott & Chedin, 1981) and surface emissivity spectra of the ASTER spectral library (Baldridge, et al., 2009).

2 METHODOLOGY

2.1 Split window algorithm improvement

Considering each thermal spectral impact of both the ground and atmosphere at the remote sensor level, the general RTE (Otlle & Stoll, 1993) for LST retrieval can be formulated as

$$B_i(T_i) = \tau_i(\theta)[\varepsilon_i B_i(T_s) + (1-\varepsilon_i)L_i^{\downarrow}] + L_i^{\uparrow} \quad (1)$$

where T_s is LST, T_i is the at-sensor BT in thermal channel i, $\tau_i(\theta)$ is the atmospheric transmittance in channel i at VZA θ, and ε_i is the ground emissivity. $B_i(T_i)$ and $B_i(T_s)$ is the Planck radiances of the at-sensor and surface, and $L_i^{\downarrow}$ and $L_i^{\uparrow}$ are the downward and upward radiances, respectively. Qin, et al.(2001) identify a derivation of $L_i^{\uparrow}$ and $L_i^{\downarrow}$, described below

$$L_i^{\uparrow} = (1-\tau_i(\theta'))B_i(T_a)$$
$$L_i^{\downarrow} = (1-\tau_i(\theta))B_i(T_a^{\downarrow}) \quad (2)$$

where $T_a^{\uparrow}$ and $T_a^{\downarrow}$ is the effective atmospheric average temperatures of the upward and downward radiance. θ' is the downward direction of atmospheric radiance. Using $L_i^{\uparrow}$ and $L_i^{\downarrow}$, Eq.(1) can be expressed below

$$B_i(T_i) = \tau_i(\theta)[\varepsilon_i B_i(T_s) + (1-\varepsilon_i)(1-\tau_i(\theta))B(T_a^{\downarrow})] + (1-\tau_i(\theta'))B_i(T_a) \quad (3)$$

To simplify Eq.(3), Qin, et al.(2001) and Mao, et al.(2005) made some simplifications and provided two assumptions that do not have much influence on LST retrieval accuracy if $T_a^{\uparrow}=T_a^{\downarrow}$ and $\tau_i(\theta)=\tau_i(\theta')$, such as in Eq.(4).

$$B_i(T_i) = \tau_i(\theta)\varepsilon_i B_i(T_s) + (1-\tau_i(\theta))[1+(1-\varepsilon_i)\tau_i(\theta)]B_i(T_a^{\uparrow}) \quad (4)$$

Although the first assumption does not affect LST retrieval accuracy, the second is not acceptable in the case when the VZA of pixels is far from 53°; in that case, downward radiance largely differs from upward radiance, thereby causing a LST retrieval error in the SWA. To reduce this error, we introduce the Optimal Path Angles (OPAs) of upward radiance with respect to downward radiance.

$$B_i(T_i) = \tau_i(\theta)[\varepsilon_i B_i(T_s) + (1-\varepsilon_i(1-\tau_i(\theta_{opa}))B_i(T_a^{\uparrow})] + (1-\tau_i(\theta))B_i(T_a^{\uparrow}) \quad (5)$$

where θ_{opa} means the OPA of upward transmittance corresponding to downward radiance in the thermal channel i.

Otherwise, in the previous algorithms, each B_i term in Eq.(5) has the same linear regressive coefficient over the whole temperature range, which may cause some error in LST due to the difference from each temperature range for T_s and T_a(Galve, et al., 2008). As known from the simulation of $T-T_s$ and $T-T_a$ using the MODTRAN4 model, T_s-T belongs to ±20 K, while $T-T_a$ has the larger difference of temperature than T_s-T. Therefore, the linearization of the Planck radiance function in the sub-temperature range is introduced below

$$B_i(T_j) = a_{ij}T_{ij} + b_{ij}$$
$$T_j \in [t_j, t_{j+i}], (t_j \in [230, 330\ \mathrm{K}], t_{j+1} - t_j = 10\ \mathrm{K}, j = \overline{1, n}) \quad (6)$$

where T_{ij} is the at-sensor BT in the j_{th} interval in channel i, n is the step number of the at-sensor BT range divided by 10 K.

By introducing the linear fit to each term of $B(T_s)$ and $B(T_a)$ to reduce the LST error due to the difference of each temperature range, we rewrite Eq.(5) as an optimal RTE with respect to T_s corresponding to every sub-temperature range for each thermal channel i as Eq.(7)

$$a_{ij}T_{ij}+b_{ij}=P_{ij}(c_{ij}T_{sj}+d_{ij})+R_{ij}(e_{ij}T_{aj}+f_{ij})$$
$$T_{sj}=(a_{ij}T_{ij}+b_{ij}-P_{ij}d_{ij}-R_{ij}(e_{ij}T_{aj}+f_{ij}))/P_{ij}c_{ij} \quad (7)$$

where T_{sj} and T_{aj} are LST, T_a according to the j_{th} interval of the at-sensor BT, respectively. The nonlinear regressive coefficients are a_{ij}, b_{ij}, c_{ij}, d_{ij}, e_{ij} and f_{ij}. P_{ij} and R_{ij} are coefficients expressed as $\tau_{ij}(\theta)\cdot\varepsilon_{ij}(\theta)$ and $\tau_{ij}(\theta)\cdot(1-\varepsilon_{ij}(\theta))\cdot(1-\tau_{ij}(\theta_{opa}))+(1-\tau_{ij}(\theta))$, respectively. Finally, an improved SWA for more accurate LST retrieval is obtained by transferring T_{aj} from two thermal channels in Eq.(7).

2.2 Water vapor content and transmittance

To retrieve TCWVC, an operational algorithm presented by Sobrino, et al. (2003) was used which uses channels 2, 17, 18 and 19 of MODIS data. We propose a method based on the simulation using the MODTRAN4 model with 875 profiles of TIGR3 database (RH < 85%) and 106 emissivity spectra of natural surfaces extracted carefully from the ASTER spectral library. First, to analyze the effective spectral radiance of specific potential channels of MODIS data, spectral specifications of the spectral response function (SRF) is needed. All the spectral parameters are averaged using SRFs on the different channels of MODIS considered in this paper. In the coefficient estimation, the exp-fit model is used for high accuracy.

The mean atmospheric water vapor contents (W) from radiance ratios (G_i) of MODIS could be obtained from Eq.(8) (Sobrino, et al., 2003):

$$W=f_{17}\cdot W_{17}+f_{18}\cdot W_{18}+f_{19}\cdot W_{19}$$
$$W_i=A_i\cdot\exp(-G_i/t_i)+y_i(i=17,18,\text{ and }19),\ G_i=L_i/L_2 \quad (8)$$

where A_i, t_i and y_i are coefficients of the exponential equation, f_{17}, f_{18}, and f_{19} are weighting functions defined as $f_i=\eta_i/\sum\eta_i$ with $\eta_i=\Delta\tau_i/\Delta W$. ΔW is the difference between the maximum and minimum water vapor content from the MODTRAN4 simulation using the TIGR3 database, and $\Delta\tau_i$ is the difference between the transmittances to the maximum and minimum water vapor content obtained in channel i (Kaufman & Gao, 1992). Coefficients are shown in Table 1.

Table 1 Coefficients of TCWVC evaluated by the exp-fit

G	y	A	t	η	f
17/2	−0.6786	245.902	0.1559	0.0424	0.1824
18/2	−0.0095	8.7570	0.1661	0.1033	0.4445
19/2	−0.1606	18.1933	0.1779	0.0867	0.3731

Eq.(8) has the advantage of simplicity in that TCWVC can be derived directly from satellite radiance measurements. For sensitivity analysis, we evaluate the standard deviation $\sigma_{Total}(W)$ of TCWVC using Eq.(9):

$$\sigma_{Total}(W)=\sqrt{\sum_{i=17}^{19}f_i\Delta W_i^2}$$
$$\Delta W_i=\left(-\frac{A_i}{t_i}\right)\cdot\exp(-G_i/t_i)\cdot\Delta G_i$$
$$\Delta G_i=\frac{\sigma[G_i(W_{max})]}{G_i(W_{min})-G_i(W_{max})} \quad (9)$$

where $\Delta W_i=\Delta G_i(\mathrm{d}W_i/\mathrm{d}G_i)$ and $\sigma[G_i]$ is the standard deviation of G_i for the surface covers considered in the simulation of channel i. Based on the error analysis of the estimated TCWVC, a standard deviation for the case of MODIS is 0.3042 g/cm^2 for a wet atmosphere (6.269 g/cm^2) and 0.0112 g/cm^2 for a dry atmosphere (0.056 g/cm^2). We also performed a comparison analysis of TCWVC error in the 0 to 1 range of water vapor amount between the quadratic and exp-fit and found that the latter was more appropriate to compute TCWVC. As shown in Table 2, owing to the property of quadratic fit model, the proportion of standard deviation error to the decrease of water vapor is not satisfied in the range near to zero.

Table 2 Differences in using two fits of mean standard deviation error between the proportional relations to the decrease of TCWVC in the range from near to zero

	Mean Std Error/(g · cm^{-2})					
TCWVC	0.056	0.088	0.163	0.298	0.494	0.686
Quadratic	0.025	0.019	0.013	0.020	0.037	0.050
Exponential	0.017	0.018	0.021	0.027	0.034	0.042

In the simulation of transmittance considering the VZA effect in the two MODIS thermal channels, the transmittances were obtained from the change in relation of transmittances to TCWVC to the VZA change of a 10° interval from 0° to 60°. Based on the evaluation of minimum error related to transmittance and TCWVC, the polynomial fit model is determined by Eq.(10) and Eq.(11):

$$\tau_i(\theta)=\sum_{j=0}^{3}f_{ij}(\sec\theta)\cdot W^j \quad (10)$$
$$f_{ij}(\sec\theta)=\sum_{k=0}^{2}A_{ijk}\cdot(\sec\theta)^k \quad (11)$$

where $\sec\theta$ is sec of VZA θ, f_{ij} is the quadratic function with respect to $\sec\theta$, and A_{ijk} is the quadratic coefficient. From the simulation of the MODTRAN4 model with 875 TIGR3 profiles, we made a list of the quadratic coefficients for MODIS 31/32 (Table 3).

Table 3 Coefficients of quadratic fit to transmittance and TCWVC related to the VZA change for MODIS 31/32

Channel	Coefficient	2-order	1-order	Constant
31	A_0	−0.00479	0.01680	−0.01039
	A_1	0.03504	−0.14546	0.08886
	A_2	−0.08054	0.28586	−0.23021
	A_3	0.04950	−0.21400	1.12870
32	A_0	−0.00202	0.01197	−0.00687
	A_1	0.02347	−0.11986	0.06615
	A_2	−0.05889	0.20912	−0.19701
	A_3	0.04103	−0.18832	1.09433

2.3 Relation of upward and downward radiances

The downward and upward radiances could be expressed as Eq.(12) with small simulation errors. Because of the negligible effect on LST retrieval, T_a and $T_a^{\uparrow}$ could be conveniently assumed as $T_a\approx T_a^{\uparrow}$ under the constant condition of VZA.

$$L\downarrow(\lambda_i) = 2\int_0^{\pi/2} L_i^{\downarrow}(\lambda,\theta)\sin\theta\cos\theta d\theta = (1-\tau_i^{\downarrow}(\theta'))B(\lambda_i,T_a)$$
$$L\uparrow(\lambda_i,\theta) = (1-\tau_i^{\uparrow}(\theta))B(\lambda_i,T_a^{\uparrow}) \quad (12)$$

From the MODTRAN4 simulation, we have shown that the total downward radiance is very similar to the downward radiance in the direction of 53° as the RMSE is 0.0591/0.065 for MODIS 31/32. For the operational utility of the downward radiance, Mao, et al. (2005) substituted the upward radiance term of Eq.(12) for the downward radiance in the RTE. It is found that the LST retrieval error is non-negligible due to the above assumption and a change in transmittance to the VZA effect should be considered. We performed an error analysis between downward radiance and upward radiance related to VZA variations to determine OPAs of upward transmittance corresponding to downward radiance using the MODTRAN4 model with the TIGR3 database in the two thermal channels. Based on the mean value theorem, Eq.(12) can be alternated with Eq.(13) in which the directional transmittance term corresponds to the transmittance part of downward radiance. From the error analysis of interrelation of downward and upward radiances, we performed the minimization process based on Eq.(14) to determine OPAs of upward transmittance in Eq.(13). In Eq.(14), θ_{opa} is 55.7° and 55.8° with respective RMSEs of 0.0652 and 0.0892 in radiance units for MODIS 31/32 (Fig.1). RMSEs of LST retrieval from the MODTRAN4 simulation are 0.048 K and 0.052 K for MODIS 31/32, respectively. Generally, the larger error trend of LST retrieval is dominated by a larger TCWVC.

$$L\downarrow(\lambda_i) \approx (1-\tau_i^{\uparrow}(\theta_{opa}))B(\lambda_i,T_a) \quad (13)$$
$$\theta_{opa} = \min_{\theta}\|L\uparrow(\lambda_i,\theta) - L\downarrow(\lambda_i)\|^2 \quad (14)$$

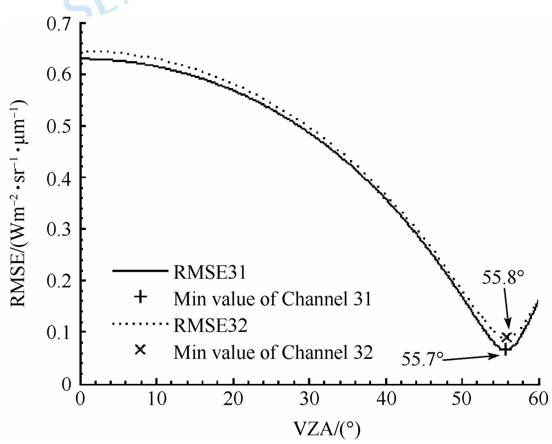

Fig.1 Determination of OPAs of upward transmittance corresponding to downward radiance using the MODTRAN4 model with TIGR3 database in MODIS 31/32

However, in the real sky conditions, the TCWVC is not large; thus, this LST error can be negligible in the accuracy estimate of the proposed algorithm.

2.4 Land surface emissivity

Given the range of arid land surface emissivity with sparse vegetation and exposed surfaces, we used an NDVI-based method (Momeni & Saradjian, 2007) to derive mean emissivity for MODIS 31/32. The NDVI-Based emissivity method is proposed using reflectivity measurements of J. H. Salisbury's spectral library and atmospherically corrected Red and Near Infrared (NIR) channels of MODIS data. The work is particularly focused on producing an emissivity estimation of 39 different soil types. As the non-correlation between water body and NDVI, the water and snow/ice types are not considered in this paper. Using these spectral data and SRFs relative to the MODIS reflective and thermal wavelengths, the reflectance of channel 1/2 and emissivity of channel 31/32 can be obtained. In atmospherically corrected MODIS-NDVI, bare soil is identified by NDVI < 0.156, partially vegetated land is identified by 0.156 ≤ NDVI ≤ 0.461 and fully vegetated area is identified by NDVI > 0.461.

For atmospherically uncorrected MODIS-NDVI, the thresholds are 0.296 and 0.615, respectively. In the implementation stage of simulated data, Pv values were calculated for each sample according to Eq.(15) (Carlson & Ripley, 1997).

$$Pv = \left[\frac{\mathrm{NDVI} - \mathrm{NDVI}_{min}}{\mathrm{NDVI}_{max} - \mathrm{NDVI}_{min}}\right]^2 \quad (15)$$

where NDVI_{min} = 0.156 and NDVI_{max} = 0.461 correspond to the NDVI threshold values of atmospherically corrected MODIS data specified for partially vegetated soil; otherwise, NDVI_{min} = 0.296 and NDVI_{max} = 0.615 for atmospherically uncorrected MODIS data.

2.5 Coefficient determination of SWA

The diverse situations with various land surfaces (emissivity) and atmospheres (LST and atmosphere temperature at the first layer) over the different VZAs are considered in the analysis of the proposed SWA to retrieve LST. The MODTRAN4 model is used to regress the algorithm coefficients (a, b, c, d, e and f). 875 profiles of TIGR3 database, 106 natural surface types of emissivity spectra from the ASTER-JHU emissivity spectral database at nadir, 7 VZAs with 10° intervals (0°—60°) and 5 T_s(T_o, T_o±10 and T_o±20) have been chosen for T_i simulation. In the forward simulation, the values of all spectral characteristics are obtained by integration of their SRFs for each channel i. Table 4 shows the estimated coefficients for the sub-ranges of temperature. When T_a is removed from the two RTEs of Eq.(7), Eq.(16) finally becomes a new operational SWA proposed for LST retrieval from the two channels (channel 1 and channel 2) of MODIS.

The definition of parameters R and P in Eq.(16) was shown in Eq.(7).

$$T_{Sj} = [e_{ch2j}R_{ch2j}(a_{ch1j}T_{ch1j} + b_{ch1j} - d_{ch1j}P_{ch1j} - f_{ch1j}R_{ch1j}) - e_{ch1j}R_{ch1j}(a_{ch2j}T_{ch2j} + b_{ch2j} - d_{ch2j}P_{ch2j} - f_{ch2j}R_{ch2j})] / (c_{ch1j}e_{ch2j}P_{ch1j}R_{ch2j} - c_{ch2j}e_{ch1j}P_{ch2j}R_{ch1j}) \quad (16)$$

As shown in Table 5, the total RMSE of LST retrieval by the proposed algorithm is 0.34 K, while RMSE is 0.65 K for Mao, et al.(2005)'s algorithm. Moreover, from the effect of LST error between downward and upward radiance relative to the change in VZA, the RMSE values from Mao, et al.(2005)'s algorithm become greater as the VZA decreases. Besides, the RMSE of LST retrieval from our algorithm is almost independent on the change of VZA.

Table 4 Coefficients of the proposed SWA when T_s equals to T_o, T_o±10 and T_o±20, and the VZA Change has 7 Angles (0° to 60°) for MODIS 31/32

At-Sensor BT/K	a (31/32)	b (31/32)	c (31/32)	d (31/32)	e (31/32)	f (31/32)	R^2_T_s (31/32)	RMSE_T_s/K (31/32)
230—240	0.07	−13.25	0.07	−13.67	0.07	−13.37	0.9995	0.06
	0.07	−12.31	0.07	−12.55	0.07	−13.39	0.9997	0.05
240—250	0.08	−15.60	0.08	−16.14	0.07	−14.32	0.9996	0.06
	0.07	−14.23	0.07	−14.54	0.07	−13.98	0.9997	0.05
250—260	0.09	−18.30	0.09	−18.97	0.08	−15.52	0.9997	0.06
	0.08	−16.40	0.08	−16.79	0.08	−15.04	0.9997	0.05
260—270	0.10	−21.19	0.10	−22.03	0.09	−17.35	0.9997	0.06
	0.09	−18.68	0.09	−19.19	0.08	−16.38	0.9998	0.05
270—280	0.11	−24.28	0.11	−25.13	0.1070	−22.98	0.9994	0.08
	0.10	−21.09	0.10	−21.68	0.0944	−19.76	0.9997	0.06
280—290	0.12	−27.55	0.13	−28.82	0.1197	−26.53	0.9991	0.11
	0.1082	−23.62	0.11	−24.72	0.1071	−23.27	0.999	0.14
290—300	0.13	−30.86	0.14	−33.49	0.1299	−29.46	0.9987	0.18
	0.12	−26.10	0.13	−28.72	0.1132	−25.04	0.9987	0.21
300—310	0.15	−34.25	0.16	−37.40	0.1337	−30.55	0.9992	0.15
	0.13	−28.61	0.13	−31.05	0.1168	−26.08	0.9991	0.17
310—320	0.16	−37.65	0.17	−40.94	0.1344	−30.74	0.9996	0.08
	0.13	−31.17	0.14	−33.74	0.1162	−25.91	0.9997	0.08
320—330	0.17	−40.87	0.18	−43.76	0.1366	−31.40	0.9999	0.02
	0.14	−33.42	0.15	−35.70	0.1166	−26.03	1.0000	0.01
Total							0.9994	0.09
							0.9994	0.10

Table 5 RMSE values of LST retrieval from two algorithms at the different VZAs using the MODTRAN4 4 Model in MODIS 31/32

VZA /(°)	Mao, et al.'s algorithm RMSE/K	Our algorithm RMSE/K
0	0.89	0.32
10	0.76	0.34
20	0.71	0.35
30	0.67	0.35
40	0.63	0.34
50	0.61	0.34
60	0.59	0.35
Total	0.65	0.34

Table 6 Characteristics of TIGR3 profiles and emissivity from the JHU spectral data for the sensitivity analysis of the proposed algorithm in MODIS 31/32

Name	TIGR3 No.	T_o/K	TCWVC/ ($g \cdot cm^{-2}$)	Type	ε_{31}	ε_{32}
T1	645	296.85	4.13	Lime	0.971	0.977
T2	795	293.85	3.01	Hornfels	0.966	0.977
T3	882	286.87	2.06	Clay	0.974	0.981
T4	1039	282.85	1.01	Loam	0.966	0.974
T5	1359	272.05	0.51	Water	0.991	0.985
T6	1692	264.05	0.19	Conifer	0.989	0.991
				Grass	0.984	0.989

3 SENSITIVITY ANALYSIS

Sensitivity analysis is necessary for taking into account the effect of LST retrieval error due to possible errors of parameter determination and assumptions in the SWA. To evaluate the sensitivity of the LST retrieval error using the MODTRAN4 model, the ground/satellite spectral radiance database was simulated with seven typical surface types from the JHU emissivity spectral database and six atmospheric profiles from the TIGR3 database (Ouyang, et al., 2010) (Table 6).

First, to evaluate the sensitivity of our algorithm to the TCWVC error at nadir, we used data in Table 6 to retrieve LST with TCWVCs ranging from 0.3 to 2.0 times of the actual value. Fig.2(a) shows errors of retrieved LST with the T3 atmosphere and seven different surface conditions when the TCWVC of T3 is changed between 0.3 and 2.0 times of the actual TCWVC value. Fig.2(b) shows errors of retrieved LST for all atmospheres (T1—T6) with TCWVC=0.1 to 2.0 times of the actual TCWVCs and a rock surface.

First, 0.3 to 2.0 times of the actual TCWVC led to an LST error of −1.2 K to 0.5 K depending on the surface types under

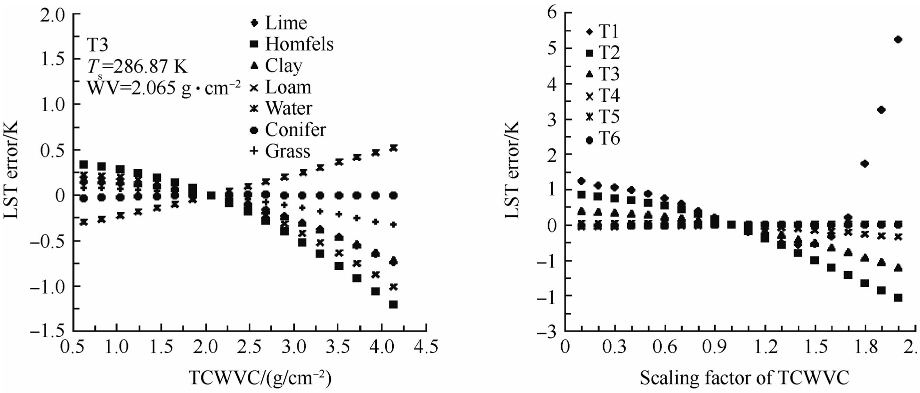

(a) T3 atmosphere (b) All atmospheric conditions (T1—T6)

Fig.2 Effect of TCWVC error on LST retrieval for the T3 atmosphere and all surface types and for all atmospheric conditions (T1—T6) and a hornfels sample

the moderately moist atmosphere (T3). The LST error was −0.51 K to 0.28 K for a rock body with more changeable spectral emissive characteristics, but −0.2 K to 0.08 K for all surface types within 50% of the actual TCWVC. Second, the LST errors for a dry atmosphere were smaller than those for a moist atmosphere. The absolute accuracy of TCWVC retrieval from the MODIS instrument ranges from −13% to 13% in the cloud-free conditions (Kaufman & Gao, 1992). Subsequently, we conclude from the above results that our algorithm is not sensitive to TCWVC for LST retrieval. Thirdly, to evaluate the sensitivity to the transmittance error of MODIS 31/32 due to the different VZAs, we performed two simulations. One simulation evaluated the LST error due to different VZA from 0° to 60° over a T3 atmosphere and all surface types in Table 6. The other simulation covered all atmospheres (T1—T6) as well as a certain surface type that affects the LST error more than other surfaces. Fig.3 shows the effects of different VZAs on LST retrieval (a) for the T3 atmosphere and all surface types and Fig.3(b) for all atmospheric conditions (T1—T6) with a conifer sample which has a relatively larger difference of LST errors on Fig.3(a).

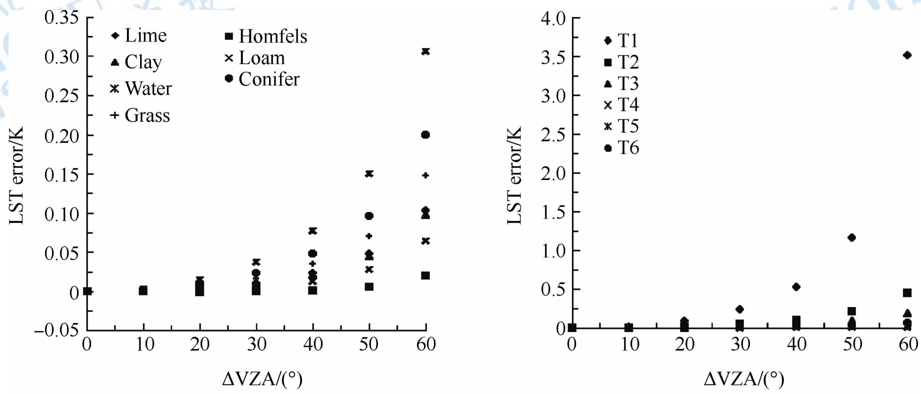

(a) T3 atmosphere (b) All atmospheric conditions (T1—T6)

Fig.3 Effect of the different VZAs on LST retrieval for the T3 atmospheric and all surface types, and for all atmospheric conditions (T1—T6) and a conifer sample surface

Fig.3(a) shows that the maximum LST error is 0.3 K for water surface, 0.2 K for vegetation and 0.1 K for rock and soil with T3 atmospheric condition. Fig.3(b) shows that the LST retrieval error is the second highest over the conifer surface for the T3 atmospheric condition. As the VZA increases to 60° the LST error increases to 3.5 K for T1 atmospheric condition, while to 0.2 K for the T3 atmospheric condition. It indicates that consideration of relationship of transmittance and VZA may reduce the overestimated LST error.

To analyze the effect of the OPAs difference, we evaluated the sensitivity of the LST error in two cases. Fig.4(a) shows the error of LST retrieved with an OPA obtained in Section 2.3 for the T3 atmospheric condition and different surface types. Fig.4(b) shows the LST error for different atmospheric conditions (T1—T6) and one land surface (hornfels sample).

The above LST error has the same tendency for every VZA, so we consider the evaluation of LST error only at the nadir in Fig.4. As shown in Fig.4(a), LST error due to the OPA difference ranged from −0.2 K to 0.2 K for the T3 atmosphere and a hornfels sample and was 0.2 K when the OPA is 0°. Moreover, it became higher in the moist atmospheric conditions in Fig.4(b). From these evaluations, we found that our algorithm that accounted for the OPAs reduced LST error caused by using the same upward transmittance as downward transmittance. Forth, we also evaluated the sensitivity of the LST retrieval error to the ground emissivity change in MODIS 31/32. Fig.5(a) shows the LST retrieval error due to the emissivity change from −0.01 to 0.008 for the T3 atmosphere across all surface types in MODIS 31.

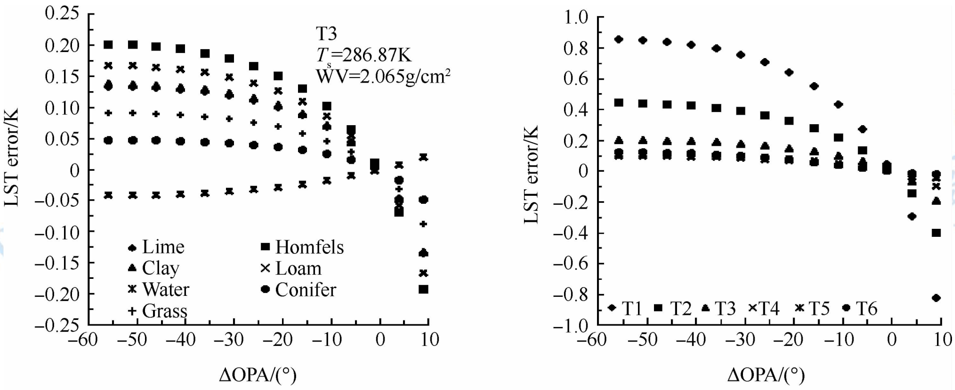

(a) T3 atmosphere (b) All atmospheric conditions (T1—T6)

Fig.4 LST error due to the OPA difference from 0° to 65° range for T3 and all surface types and for all atmospheres (T1—T6) and a hornfels sample

Fig.5(b) shows the LST error distribution with all atmospheres (T1—T6) and a hornfels sample, indicating the largest range of LST error in Fig.6(a).

Fig.6 shows the LST error from the same procedure as Fig.5, but only the emissivity of MODIS 32 changes. Fig.7 shows the LST error under the same atmospheric and surface conditions as Fig.5 when the emissivity of MODIS 31/32 changes at the same ratio.

As shown in Fig.5—Fig.7, when each emissivity changes from −0.01 to 0.008, the change in LST error for rock and soil surfaces had a very similar trend and a relatively smaller value in the moist atmospheric condition. The average LST errors changed from −0.41 K to 0.52 K and from −0.4 K to 0.5 K, respectively, in Fig.7(a) and Fig.7(b). Therefore, we concluded that our algorithm was sensitive to emissivity for most of these surface types under the moderate moist atmospheric conditions.

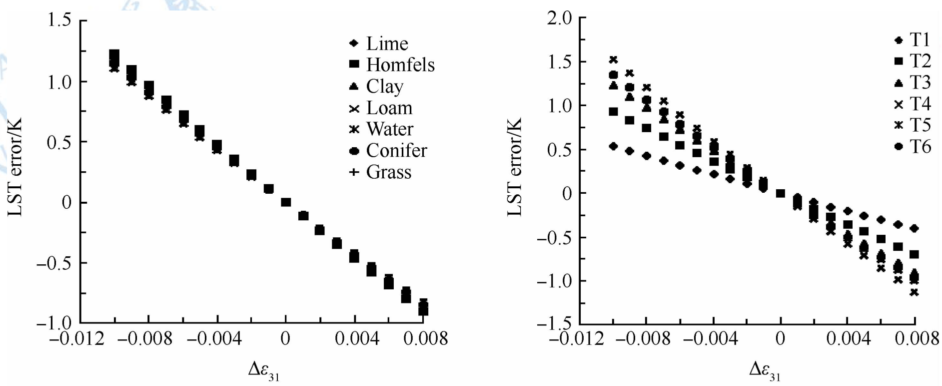

(a) T3 atmosphere (b) All atmospheric conditions (T1—T6)

Fig.5 LST error due to the emissivity change of MODIS 31 from −0.01 to 0.008 for the T3 atmosphere and all surface types and with all atmospheres (T1—T6) and a hornfels sample

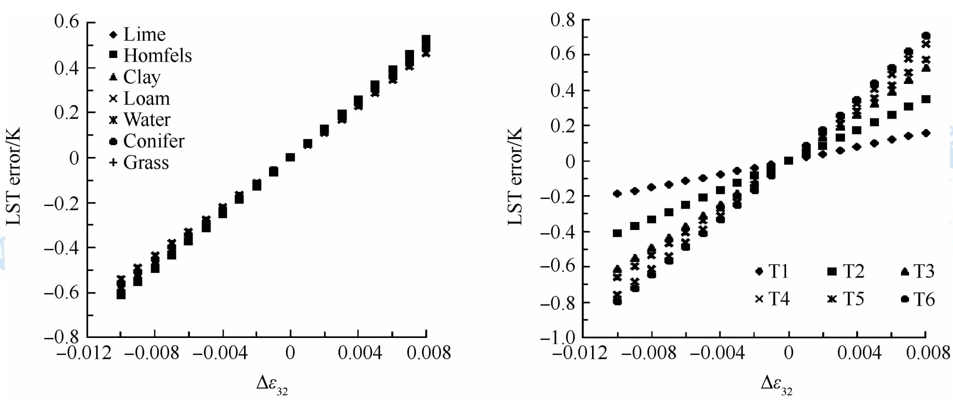

(a) T3 atmosphere (b) All atmospheric conditions (T1—T6)

Fig.6 LST error due to the emissivity change of MODIS 32 from −0.01 to 0.008 for the T3 atmosphere and all surface types and with all atmospheres (T1—T6) and a hornfels sample

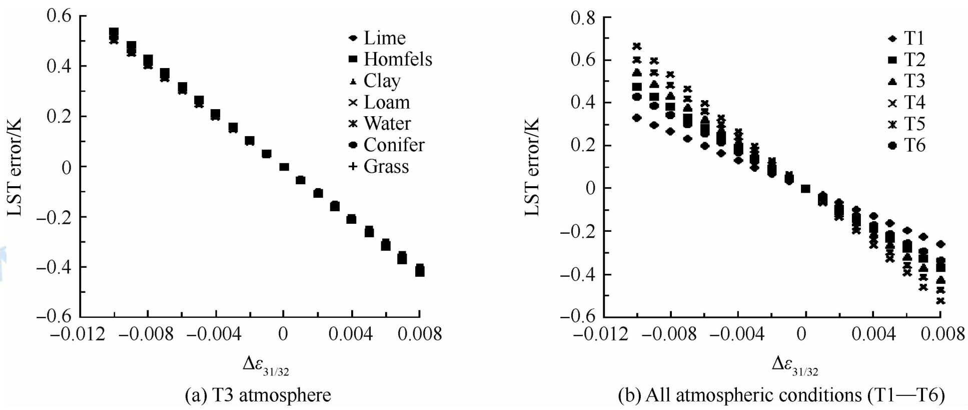

Fig.7 LST error due to the simultaneous emissivity change of MODIS 31/32 from −0.01 to 0.008 with the T3 atmosphere and all surface types and with all atmospheres (T1—T6) and a hornfels sample

4 VALIDATION

Validation sites should be on an area with large, flat and homogeneous cover for surface temperature and emissivity. Given these requirements, the SURFRAD observed surface long-wave radiation (upward and downward radiative fluxes) by a precise infrared radiometer (PIR), was selected at six sites during the entire month of June 2009.

4.1 Ground-measured temperature

Based on the thermal radiative transfer theory, LST (T_s) is related to surface emissivity and surface long-wave radiation by the Stefan-Boltzmann law (Liang, 2004) as below

$$F_u = \varepsilon_b \cdot \sigma \cdot T_s^4 + (1 - \varepsilon_b) \cdot F_d \tag{17}$$

where F_u is the surface upward longwave radiation, ε_b is the broadband LSE over the entire infrared region, σ is the Stefan-Boltzmann's constant (5.67×10^{-8}/Wm^{-2}K^{-4}), and F_d is atmospheric downward long-wave radiation at the surface. MODIS-UCSB and ASTER-JHU spectral libraries were used for the estimation of the broadband LSE ε_b denoted as

$$\varepsilon_b = \frac{\int_{\lambda=\lambda_1}^{\lambda=\lambda_2} \varepsilon(\lambda) B(\lambda, T_s)\,d\lambda}{\int_{\lambda=\lambda_1}^{\lambda=\lambda_2} B(\lambda, T_s)\,d\lambda} \tag{18}$$

where $B(\lambda, T_s)$ denotes the emitted radiance given by Planck's radiance at the surface temperature T_s at wavelength λ, and $\lambda_1 \approx 3$ μm and $\lambda_2 \approx 14$ μm are the lower and upper limit spectral wavelength values, respectively. The three dry grass samples available from the MODIS-UCSB library were employed to better characterize this type of surface because there is only one grass sample in the JHU library. Meanwhile the assumption of a constant value for (e.g., $T_s = 300$ K) did not induce significant error because the temperature dependence of LSE is usually very small for most surface types. In fact, for both grass spectral library data of the JHU and MODIS-UCSB varying in the range of T_s(240—320 K), the variations of ε_b are less than 0.007; thus, in Eq.(18), it can be assigned T_s for 300 K.

4.2 Validation against ground-measured temperature

To evaluate the accuracy of the LST estimated from the above method, we compared the three results of MODIS LST retrievals with the 104 SURFRAD measurements at six sites during the month of June 2009 when the inherent spectral information of land covers is well presented (Yu, et al., 2012). Table 7 lists the station ID of SURFRAD measured sites. From ground-measured long-wave radiations, ground-measured LSTs from SUFRAD data can be obtained using Eq.(17).

Table 7 List of SURFRAD measurement sites

Site No.	Site location	Latitude/(°N) Longitude/(°W)	Land cover type
1	Bondville, IL	40.05/88.37	Crop
2	Fort Peck, MT	48.31/105.10	Grass
3	Goodwin Creek, MS	34.25/89.87	Deciduous Forest
4	Table Mountain, CO	40.13/105.24	Crop
5	Desert Rock, NV	36.62/116.02	Open shrub
6	Pennsylvania State University, PA	40.72/77.93	Mixed forest

The error statistics of LST retrieval against the ground measurements are shown in Table 8. Bias and RMSE represent mean difference and RMSE between MODIS retrieved LSTs and SURFRAD measurements, and N indicates the total sample numbers. Subscript "MOD11", "Mao" and "New" indicate the abbreviations of MOD11 _ L2 LST, previous LST and our proposed LST, respectively.

Table 8 Comparison of ground and LSTs derived from MODIS data

Site No.	Number	Bias/K			RMSE/K		
		MOD11	Mao	New	MOD11	Mao	New
1	14	−0.71	1.14	−0.51	0.86	1.46	0.72
2	20	−0.38	1.33	−0.69	0.99	1.48	1.09
3	19	−0.71	1.29	−0.79	0.86	1.36	0.98
4	15	−0.38	1.33	−0.69	0.99	1.48	1.09
5	19	−0.41	1.66	−0.79	1.28	1.77	0.96
6	17	−0.47	1.29	−0.41	0.82	1.43	0.77
Sum	104	−0.38	1.34	−0.66	1.0	1.49	0.93

LST results retrieved from our proposed algorithm agreed well with the ground measurements, with an RMSE of 0.93 K, while MOD11_L2 LST and Mao, et al.(2005)'s LST have RMSEs of 1 K and 1.49 K, respectively. The bias of LST retrieved by our algorithm was −0.66 K. Table 8 shows that the LSTs retrieved from our method are more similar to MODIS_L2 LSTs with a mean bias of −0.38 K and −0.66 K, respectively. However, LST retrieved by Mao, et al.(2005)'s algorithm greatly differs from MODIS_L2 LST, with a bias of 1.34 K. One reason for this LST error may be the estimation of atmospheric parameters without considering the VZA effect and the linearization of the Planck radiance function in the whole range of the at-sensor BT. Another reason is the use of spectral emissivity of dry grass samples in the MODIS-UCSB library instead of the ground broadband emissivity measured directly for the ground-measured LSTs, such that during the time of measurement, the ground-measured LSTs at a test site could be different from the satellite-derived LST. As a result, our proposed algorithm can retrieve LSTs more accurately than Mao, et al.(2005)'s algorithm from Terra/MODIS data.

5 CONCLUSION

In this paper, an improved method to retrieve LST from Terra/MODIS data using the SWA at daytime is presented. From the MODTRAN4 simulation with 875 profiles of TIGR3, 106 emissivity spectral library data and seven VZAs, the atmospheric parameters (TCWVC and transmittances of two adjacent thermal channels) considering the effect of VZA change were determined. The OPA of directional transmittances in MODIS 31/32 between the downward and upward radiances has been estimated as 55.7° and 55.8° with an RMSE of 0.048 K and 0.052 K, respectively. Based on every range of the at-sensor BT, linear coefficients of at-surface and effective atmospheric Planck radiances corresponding to sub-ranged at-sensor BT were also estimated from the MODTRAN4 simulation. The RMSE value of LST retrieval using our proposed algorithm was 0.34 K, while the RMSE value of LST retrieval was 0.65 K for Mao, et al.(2005)'s algorithm from the MODTRAN4 simulation. Moreover, from the effect of the difference between downward and upward radiance relative to a change in VZA, RMSE values from Mao, et al.(2005)'s algorithm became greater as the VZA change decreased. On the other hand, LST retrieval error from our algorithm was nearly independent on the change in VZA. According to sensitivity analyses, our algorithm was not sensitive to TCWVC and ground emissivity for the moderate moist atmospheric conditions and LST retrieval error due to the VZA difference was thus reduced. With the SURFRAD measurements at six sites, during the month of June 2009, the accuracy of LST retrieval from the proposed algorithm was compared with that of Mao, et al.(2005)'s LST and MOD11_L2 LST. The RMSE values of LST were 0.93 K for our proposed method, 1.49 K from Mao, et al.(2005)'s algorithm and 1 K for MOD11_L2 LST product, respectively, while the average biases were −0.66 K, 1.34 K and −0.38 K, respectively. As a result, the proposed algorithm provides more accurate LST retrieval than Mao, et al.'s algorithm and MODIS_L2 LST product. In the future, for the refinement of LST retrieval from our proposed algorithm, the study of directional emissivity estimation toward VZA and validation with more ground-measured data should be performed.

REFERENCES

Atitar M and Sobrino J A. 2009. A split-window algorithm for estimating LST from Meteosat 9 data: test and comparison with in situ data and MODIS LSTs. IEEE Geoscience and Remote Sensing Letters, 6(1): 122−126[DOI: 10.1109/LGRS.2008.2006410]

Baldridge A M, Hook S J, Grove C I and Rivera G. 2009. The ASTER spectral library version 2.0. Remote Sensing of Environment, 113(4): 711−715[DOI: 10.1016/j.rse.2008.11.007]

Carlson T N and Ripley D A. 1997. On the relation between NDVI, fractional vegetation cover, and leaf area index. Remote Sensing of Environment, 62(3): 241−252[DOI: 10.1016/S0034−4257(97)00104−1]

Coll C and Vicente C. 1997. A split-window algorithm for land surface temperature from advanced very high resolution radiometer data: validation and algorithm comparison. Journal of Geophysical Research, 102(D14): 16697−16713[DOI: 10.1029/97JD00929]

Galve J M, Coll C, Caselles V and Valor E. 2008. An atmospheric radiosounding database for generating land surface temperature algorithms. IEEE Transactions on Geoscience and Remote Sensing, 46(5): 1547−1557 [DOI: 10.1109/TGRS.2008.916084]

Jedlovec G J. 1990. Precipitable water estimation from high-resolution split window radiance measurements. Journal of Applied Meteorology and Climatology, 29(9): 863−876 [DOI: 10.1175/1520−0450(1990)029<0863:PWEFHR>2.0.CO;2]

Jiang G M and Li Z L. 2008. Split-window algorithm for land surface temperature estimation from MSG1-SEVIRI data. International Journal of Remote Sensing, 29(20): 6067−6074 [DOI: 10.1080/01431160802235860]

Kaufman Y J and Gao B C. 1992. Remote sensing of water vapor in the near IR from EO S/MODIS. IEEE Transactions on Geoscience and Remote Sensing, 30(5): 871−884[DOI: 10.1109/36.175321]

Li Z L and Becker F. 1993. Feasibility of land surface temperature and emissivity determination from AVHRR data. Remote Sensing of Environment, 43(1): 67−85 [DOI: 10.1016/0034−4257(93)90065−6]

Liang S L. 2004. Quantitative Remote Sensing of Land Surfaces // Kong J A, ed. Wiley Series in Remote Sensing. Jew Jersey: John Wiley & Sons

Mao K B, Qin Z, Shi J and Gong P. 2005. A practical split-window algorithm for retrieving land surface temperature from MODIS data. International Journal of Remote Sensing, 26(15): 3181−3204 [DOI: 10.1080/01431160500044713]

Momeni M and Saradjian M R. 2007. Evaluating NDVI-based emissivities of MODIS bands 31 and 32 using emissivities derived by Day/Night LST algorithm. Remote Sensing of Environment, 106(2): 190−198 [DOI: 10.1016/j.rse.2006.08.005]

Otlle C and Stoll M. 1993. Effect of atmospheric absorption and surface emissivity on the determination of land surface temperature from infrared satellite data. International Journal of Remote Sensing, 14(10): 2025−2037 [DOI: 10.1080/01431169308954018]

Ouyang X, Wang Y, N, Wu H and Li Z L. 2010. Errors analysis on temperature and emissivity determination from hyperspectral thermal infrared data. Optics Express, 18(2): 544−550 [DOI: 10.1364/OE.18.000544]

Qin Z H, Dall'Olmo G, Karnieli A and Berliner P. 2001. Derivation of split window algorithm and its sensitivity analysis for retrieving land surface temperature from NOAA-advanced very high resolution radiometer data. Journal of Geophysical Research, 106(D19): 22655−22670 [DOI: 10.1029/2000JD900452]

Scott N A and Chedin A. 1981. A fast line by line method for atmospheric absorption computations: the Automatized Atmospheric Absorption Atlas. Journal of Applied Meteorology, 20(7): 802-812 [DOI: 10.1175/1520-0450(1981)020<0802:AFLBLM>2.0.CO;2]

Sobrino J A, Li Z L, Stoll M P and Becker F. 1996. Multi-channel and multi-angle algorithms for estimating sea and land surface temperature with ATSR data. International Journal of Remote Sensing, 17(11): 2089-2114 [DOI: 10.1080/01431169608948760]

Sobrino J A, Kharraz J E. and Li Z L 2003. Surface temperature and water vapour retrieval from MODIS data. International Journal of Remote Sensing, 24(24): 5161-5182 [DOI: 10.1080/0143116031000102502]

Tang B H, Bi Y Y, Li Z L and Xia J. 2008. Generalization split-window algorithm for estimate of land surface temperature from Chinese geostationary Fengyun meteorological satellite (FY-2c) data. Sensors, 8(2): 933-951 [DOI: 10.3390/s8020933]

Yu Y Y, Tarpley D, Privette J L, Flynn L E, Xu H, Chen M, Vinnikov K Y, Sun D L and Tian Y H. 2012. Validation of GOES-R satellite land surface temperature algorithm using SURFRAD ground measurements and statistical estimates of error properties. IEEE Transactions on Geoscience and Remote Sensing, 50(3): 704-713 [DOI: 10.1109/TGRS.2011.2162338]

Yu Y Y, Tarpley D, Privette J L, Goldberg M D, Rama Varma Raja M K, Vinnikov K Y and Xu H. 2009. Developing algorithm for operational GOES-R land surface temperature product. IEEE Transactions on Geoscience and Remote Sensing, 47(3): 936-951 [DOI: 10.1109/TGRS.2008.2006180]

Wan Z, Zhang Y, Zhang Q and Li Z L. 2004. Quality assessment and validation of the MODIS global land surface temperature. International Journal of Remote Sensing, 25(1): 261-274 [DOI: 10.1080/0143116031000116417]

Wan Z M and Dozier J. 1996. A generalized split-window algorithm for retrieving land-surface temperature from space. IEEE Transactions on Geoscience and Remote Sensing, 34(4): 892-905 [DOI: 10.1109/36.508406]

Wan Z M and Li Z L. 1997. A physics-based algorithm for retrieving land-surface emissivity and temperature from EOS/MODIS data. IEEE Transactions on Geoscience and Remote Sensing, 35(4): 980-996 [DOI: 10.1109/36.602541]

Wan Z M, Zhang Y L, Zhang Q C and Li Z L. 2002. Validation of the land-surface temperature products retrieved from Terra Moderate Resolution Imaging Spectroradiometer data. Remote Sensing of Environment, 83(1-2): 163-180 [DOI: 10.1016/S0034-4257(02)00093-7]

针对 Terra/MODIS 数据的改进分裂窗地表温度反演算法

Ri Changin[1,2]，柳钦火[1]，历华[1]，方莉[1]，YU Yunyue[3]，SUN Donglian[4]

1.遥感科学国家重点实验室 中国科学院遥感与数字研究所，北京 100101;
2.朝鲜科学院遥感与地理信息研究所 数字图像处理实验室，朝鲜;
3.美国国家海洋和大气管理局 国家环境卫星、数据与信息服务中心，美国;
4.乔治梅森大学 地理与地理信息科学系，美国

摘 要：针对 Terra/MODIS 数据提出改进的分裂窗地表温度反演算法。充分考虑了传感器观测角度(VZA)的影响,并对地表和有效大气辐射按照不同的亮度温度区间分别进行 Planck 函数简化。利用 TIGR3 大气廓线库中的 875 条晴空大气廓线,ASTER 波谱库中的 106 条地物发射率波谱,结合 MODTRAN4 大气辐射传输模型模拟得到分裂窗算法系数。利用 MODTRAN4 模拟数据对算法精度进行验证,结果表明本文的改进算法和原算法的均方根误差 RMSE 分别为 0.34 K 和 0.65 K。敏感性分析表明,在中等湿润的大气条件下,算法对大气水汽含量并不敏感。该算法降低了传感器观测角度带来的地表温度反演误差。利用 2009 年 6 月美国 SURFRAD 辐射观测网 6 个站点的实测数据对改进算法、原算法以及 MOD11_L2 地表温度产品进行了对比验证,RMSE 分别是 0.93 K、1.49 K 和 1.0 K,表明本文算法可以提高反演精度。

关键词：地表温度,分裂窗算法,MODIS,SURFRAD

中图分类号：TP79 **文献标志码：**A

引用格式：Ri Changin,柳钦火,历华,方莉,YU Yunyue,SUN Donglian. 2013. 针对 Terra/MODIS 数据的改进分裂窗地表温度反演算法. 遥感学报,17(4):830–840

Ri C G, Liu Q H, Li H, Fang L, Yu Y Y and Sun D L. 2013. Improved split window algorithm to retrieve LST from Terra/MODIS data. Journal of Remote Sensing, 17(4): 830–840 [DOI: 10.11834/jrs.20132146]

收稿日期：2012-04-28;**修订日期：**2013-03-22;**优先数字出版日期：**2013-03-29

基金项目：国家自然科学基金(编号:40730525,41101325,41171282);国家高技术研究发展计划(863 计划)(编号:2012AA12A304);欧盟第七框架项目(CEOP/AEGIS)(Call FP7-ENV-2007-1 212921)

第一作者简介：Ri Changin(1972—),男,博士,研究领域为地表辐射与温度反演。E-mail: richangin@gmail.com

通信作者简介：柳钦火(1968—),男,博士,研究员。主要研究方向包括:遥感辐射传输机理、实验与建模,典型地物波谱知识库,遥感信息时空尺度效应与模型同化。发表学术论文 140 余篇,其中 SCI 论文 30 余篇。E-mail: qhliu@irsa.ac.cn

遥感学报　启功先生创刊题名

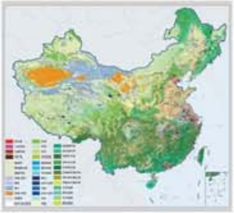

封面说明

About the Cover

2010年中国土地覆被遥感监测数据集（ChinaCover2010）

The China National Land Cover Data for 2010 (ChinaCover2010)

2010 年中国土地覆被遥感监测数据集（ChinaCover2010）由中国科学院遥感与数字地球研究所联合其他 9 个单位历时两年完成，应用 30 m 空间分辨率的环境星（HJ-1A/1B）数据，利用联合国粮农组织（FAO）的 LCCS 分类工具，构建了适用于中国生态特征的 38 类土地覆被分类系统，采用基于超算平台的数据预处理、面向对象的自动分类、地面调查获得的 10 万个野外样本以及雷达数据辅助分类相结合的方法，数据精度达到 85%。ChinaCover2010 主要基于国产卫星影像，将遥感与生态紧密结合，充足的野外样点以及严格的产品质量控制在最大程度上保证了数据的精度，可为中国生态环境变化评估以及生态系统碳估算提供基础数据支撑。（网址：http://www.chinacover.org.cn）

The China National Land Cover Data for 2010 (ChinaCover2010) has been completed after two years of team effort by the Institute of Remote Sensing and Digital Earth (RADI), Chinese Academy of Sciences (CAS), together with nine other institutions' participation. The HJ-1A/1B satellite at 30 m resolution is main data source. Based on the landscape features in China, 38 land cover classes have been defined using UN FAO Land Cover Classification System (LCCS). Super computers were used in the data preprocessing. An object-oriented method and a thorough field survey (about 100000 field samples) were used in the land cover classification, with radar imagery as auxiliary data. The overall accuracy of ChinaCover2010 is around 85%. Mainly based on domestic imagery, the products take advantage of various in situ data and strict quality control. ChinaCover2010 is a good dataset for ecological environment change assessment and terrestrial carbon budget studies. (Website: http://www.chinacover.org.cn)

遥感学报

JOURNAL OF REMOTE SENSING

YAOGAN XUEBAO（双月刊　1997年创刊）

(Bimonthly, Started in 1997)

第17卷　第4期　2013年7月25日

Vol.17 No.4 July 25, 2013

主　管	中国科学院	Superintended by	Chinese Academy of Sciences
主　办	中国科学院遥感与数字地球研究所 中国地理学会环境遥感分会	Sponsored by	Institute of Remote Sensing and Digital Earth,CAS The Associate on Environment Remote Sensing of China
主　编	顾行发	Editor-in-Chief	GU Xing-fa
编　辑	《遥感学报》编委会 北京市安外大屯路中国科学院遥感与数字地球研究所 邮编：100101　电话：86-10-64806643 http://www.jors.cn E-mail:jrs@irsa.ac.cn	Edited by	Editorial Board of Journal of Remote Sensing Add: P.O.Box 9718, Beijing 100101, China Tel: 86-10-64806643 http://www.jors.cn E-mail: jrs@irsa.ac.cn
出　版	科学出版社	Published by	Science Press
印刷装订	北京科信印刷有限公司	Printed by	Beijing Kexin Printing Co. Ltd.
总发行	科学出版社 北京东黄城根北街16号 邮政编码：100717 电话：86-10-64017032 E-mail:sales_journal@mail.sciencep.com	Distributed by	Science Press Add: 16 Donghuangchenggen North Street, Beijing 100717, China Tel: 86-10-64017032 E-mail: sales_journal@mail.sciencep.com
国外发行	中国国际图书贸易总公司 北京 399 信箱　邮政编码：100044	Overseas distributed by	China International Book Trading Corporation Add: P.O.Box 399, Beijing 100044, China

中国标准连续出版物号：ISSN 1007-4619 / CN 11-3841/TP　国内邮发代号：82-324　定价：70. 00元

CODEN YXAUAB　国外发行代号：BM 1002

ISSN 1007-4619

国内外公开发行